J Forensic Sci, Sept. 2005, Vol. 50, No. 5
Paper ID JFS2005023
Available online at: www.astm.org

Christian Jackowski,[1] *M.D.; Martin Sonnenschein,*[2] *M.D.; Michael J. Thali,*[1] *M.D.; Emin Aghayev,*[1] *M.D.; Gabriel von Allmen*[2]*; Kathrin Yen,*[1] *M.D.; Richard Dirnhofer,*[1] *M.D.; and Peter Vock,*[2] *M.D.*

Virtopsy: Postmortem Minimally Invasive Angiography Using Cross Section Techniques—Implementation and Preliminary Results*

ABSTRACT: Postmortem investigation is increasingly supported by Computed Tomography (CT) and Magnetic Resonance Imaging (MRI). This led to the idea to implement a noninvasive or minimally invasive autopsy technique. Therefore, a minimally invasive angiography technique becomes necessary, in order to support the vascular cross section diagnostic. Preliminary experiments investigating different contrast agents for CT and MRI and their postmortem applicability have been performed using an ex-vivo porcine coronary model. MSCT and MRI angiography was performed in the porcine model. Three human corpses were investigated using minimally invasive MSCT angiography. Via the right femoral artery a plastic tube was advanced into the aortic arch. Using a flow adjustable pump the radiopaque contrast agent meglumine-ioxithalamate was injected. Subsequent MSCT scanning provided an excellent anatomic visualization of the human arterial system including intracranial and coronary arteries. Vascular pathologies such as calcification, stenosis and injury were detected. Limitations of the introduced approach are cases of major vessel injury and cases that show an advanced stage of decay.

KEYWORDS: forensic science, postmortem angiography, forensic radiology, digital autopsy, virtopsy, minimally invasive autopsy, postmortem imaging, imaging autopsy, computed tomography, magnetic resonance imaging

Postmortem investigation is increasingly supported by Computed Tomography (CT) and Magnetic Resonance Imaging (MRI) (1–14). The convincing results led to the idea to implement a noninvasive or minimally invasive autopsy technique as an alternative to forensic autopsy in selected cases. This also reduces the emotional stress of the next of kin of the deceased compared to the imagination of a destructive autopsy. Furthermore, and in contrast to autopsy the acquired data can easily be stored in an objective manner and may answer newly arisen questions even decades later. Unfortunately, visualization of the pathologies of the vascular system remains a challenge.

Postmortem angiography has a long history and there are several approaches of the postmortem visualization of pathologies within the vascular system. 2D X-ray projection angiograms using barium sulfate solutions (15–18), gelatine barium suspensions (19–24), silicone rubber charged with lead oxide (25–36), gastrografin (37) or iodinated contrast agents (38,39) were used to answer specific questions regarding the vascular system. In 2001, Rah et al. (40) presented the first postmortem 3D coronary angiogram using electron-beam computed tomography. Common ground of the entire literature concerning postmortem angiography is that they are based on invasive preparation techniques and selective intubation of the vascular system to be examined and therefore depend on a traditional autopsy.

The aim of the Virtopsy® project in Bern (1) is to implement minimally invasive autopsy for postmortem investigations. In contrast to the previously published literature this paper presents a minimally invasive three-dimensional visualization of the human arterial system using Multislice Computed Tomography (MSCT).

Material and Methods

Porcine Model

Preliminary experiments to visualize arteries using MSCT and MRI as well as the micro vascular circulation using MRI were carried out on the coronary artery system of an ex-vivo porcine model. The specimens were received from a local slaughterhouse. Dissection contained the preparation of the aortic root and the ligature of all further major vessels to avoid leakage of the tested contrast agents, which might cause epicardiac artifacts.

Two series of four hearts each were investigated using MSCT. Therefore the aortic root was intubated via the brachiocephalic artery with a bulbous probe and tightly closed by several enlacements (Fig. 1*a*). The prepared hearts were placed in plastic bags to avoid contamination of the radiological equipment. Then, a native MSCT scan was performed. Prior to the injection of the contrast medium, the air within the heart due to the slaughtering procedure was extracted via the probe using a conventional syringe. 100–120 mL of the contrast agent meglumine-ioxithalamate (Telebrix®) concentrations ranging from 1% to 20% or a radiopaque barium

[1] Institute of Forensic Medicine, University of Bern, Bühlstr. 20, 3012 Bern, Switzerland.
[2] Institute of Diagnostic Radiology, University of Bern, Inselspital, 3012 Bern, Switzerland.
* Paper already presented in part at the Radiological Society of North America, 90th Scientific Assembly and Annual Meeting, November 2004, Chicago, IL.
Received 22 Jan. 2005; and in revised form 30 March 2005; accepted 9 April 2005; published 3 Aug. 2005.

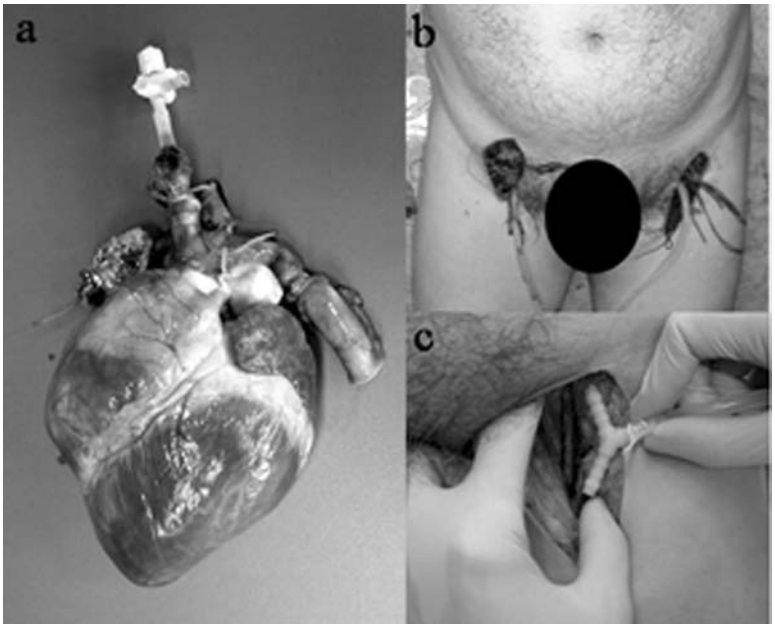

FIG. 1—*Vascular access in porcine and human corpse model: (a) Preparation of the porcine hearts with a plastic bulbous probe in the supravalvular ascending aorta and a three-way stopcock. Further vessels have been ligated or tightly sutured. (b) Angiography of the whole human corpse was performed via a small inguinal incision to get access to the right common femoral artery. The tube was advanced into the aortic arch in guide wire technique. (c) Using a T-piece within the left common femoral artery a pressure control during injection could be performed without cutting the left leg off the angiography.*

sulfate suspension (Micropaque®) were injected. MSCT scanning was performed on a 16 row scanner (Sensation 16, Siemens) with a collimation of 16 × 0.75 mm, calculated slice thickness of 0.8 mm and an increment of 0,3 mm. Postprocessing was performed on a workstation (Advantage Windows 4.1, General Electric Co., Milwaukee, WI).

For MRI the procedure remained the same except for a gadolinium based T1 shortening contrast agent (Dotarem®) in an aqueous solution replacing the X-ray contrast agent. Two series of 4 hearts each were investigated. Injected concentrations ranged from 0.1% to 1%. MR scanning was performed on a 1.5 Tesla system (Magnetom Sonata, Siemens) and sequences were as follows: axial T1-weighted (tse, TE-17 ms/TR-656 ms, flip angle 180°, slice thickness 3 mm) and flair 3D (TE-1.4 ms/TR-3.8 ms, flip angle 25°, slice thickness 1 mm) for high resolution images.

To visualize the intra myocardial micro vessels by MRI the preparation differed as follows: in a series of two hearts the aortic root was dissected and the coronary orifice of the left coronary artery was intubated with a smaller bulbous probe and tightly ligated. Injection of the gadolinium at a concentration of 0.5% was thereby limited to the myocardium fed by the left main coronary artery. MRI scanning was performed on a 1.5 Tesla Signa Echospeed Horizon unit (version 5.8, General Electric Medical Systems, Milwaukee, WI) and the sequence was used as follows; axial T1-weighted fat saturated (TE-15 ms/TR-400 ms, slice thickness 4 mm, gap 1 mm).

Human Corpse Model

Three non-fixed corpses were investigated using MSCT in close collaboration with the Institute of Human Anatomy of the University of Bern. These came from persons who had dedicated their bodies for science and education. To visualize the human arterial system including the coronary arteries in a minimally invasive way, both common femoral arteries were dissected in supine position. Using the Seldinger technique, a rigid guide wire was placed into the aortic arch via the right femoral artery. Via the guide wire, a flexible tube of the maximal possible diameter ranging from 5 mm to 8 mm was placed into the aortic arch and closed with a clamp. The tube was fixed to the femoral artery by several ligating enlacements. Two of the three human cases showed severe atherosclerosis of the iliac arteries, complicating the placing of the tube. In these cases the problem was solved by simultaneous use of an intravascular catheter and a more flexible guide wire. After having placed the catheter correctly, the flexible guide wire was replaced by a backup guide wire of distinctively lower flexibility. The catheter was then removed and the backup guide wire was used to place the flexible tube into the aortic arch.

A T-piece was inserted into the left femoral artery (Fig. 1*c*) and tightly fixed to observe the intravascular pressure while the injection of the contrast agent was performed. A conventional manometer was connected to the third access of the T-piece after the air within the system was removed. The preparation was performed at the autopsy room and afterwards the corpse was wrapped into two body bags that had been proven to cause no imaging artifacts. The tubes left the body bags via two small incisions. For the radiological investigation the corpse was transported to the Institute of Diagnostic Radiology, Inselspital, University of Bern.

At the MSCT scanning room, the injection tube was connected to the tube from the flow adjustable injection pump (COBE perfusion system, Lakewood, CO) as used in heart-lung machines. The injection system was completely filled with contrast medium to ensure that no air was within the system or could enter it. Postmortem whole body angiography was performed using an aqueous solution of meglumine-ioxithalamate at a concentration of 20%.

The radiological examination started with a native scan. Thereby arterial calcifications could be detected. The contrast agent was injected on the scanner table (Fig. 2*b*). We started with 15–20 mL/kg body weight. The injection flow was adapted to vital conditions of a regular cardiac output and was limited by an intravascular pressure threshold of 50–60 mmHg. The flow was slowly increased to a maximum of 3–4 L/min resulting in an injection time of 40–60 sec.

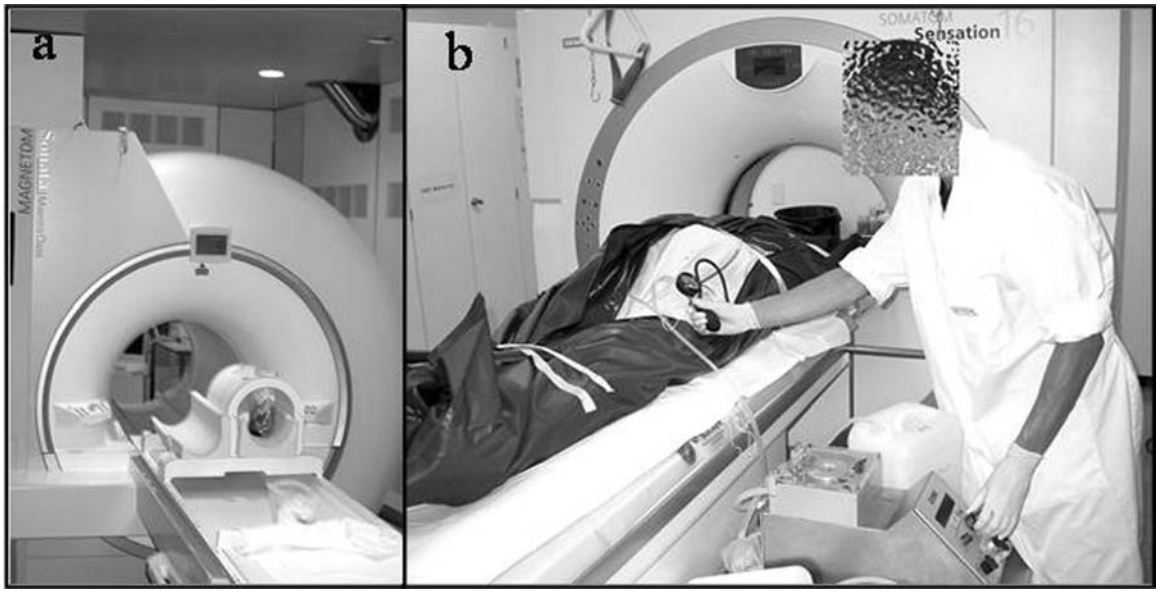

FIG. 2—*Scanning positioning in porcine and human model: (a) For MR-examination the porcine heart was placed in a conventional knee coil (usually used for MR examinations of the extremities). Injection of the gadolinium solution was performed via a to the three-way stopcock connected tube. (b) Setting of the whole corpse wrapped twice for angiography using MSCT. The flexible tubes were allowed to leave the wrapping bags. Injection prior to scanning was performed using a flow adjustable pump. The intravascular pressure was observed using a conventional manometer.*

Scanning was started immediately after the end of injection before a collapse of the vessels was possible. A second or even a third injection with subsequent scanning was performed when gas bubbles occurred within the vascular system to displace the gas and to differentiate these artifacts. The time needed for preparation of the corpses, logistics, injection and scanning ranged from 2 to 3 h. Postprocessing of the MSCT data was performed on the same workstation as within the porcine model.

After angiographic investigation, the corpses were partly dissected to validate postmortem angiographic findings.

Results

Porcine Model

The ex-vivo porcine model, MSCT and meglumine-ioxithalamate provided for an excellent visualization of the coronary artery system, without selective intubation of the coronary orifices (Fig. 3). Concentrations above 10% were useful for MSCT. MRI results were inferior to MSCT because of the increased slice thickness, but nevertheless sufficient to display the three main coronary arteries in adequate quality using a 1% aqueous solution of the administered gadolinium (Fig. 4*a*). Selective intubation of the left main coronary artery visualized the perfused myocardium in good distinction to the remaining myocardium on axial T1-weighted images (Fig. 4*b*).

Human Corpse

Postmortem angiography of the human corpse was successful in visualizing the human arterial system including e.g., the intracranial arteries. A complete visualization of the arterial circle of Willis as well as its branches is exemplarily shown in Fig. 5 and is displayed in more detail than routine autopsies do. 3D reconstructed models allow for easy stenosis detection as seen in Fig. 6. Minimally invasive coronary angiography also became possible (Fig. 7). The main coronary branches became visualized and allowed for calcified plaque detection and for an assessment of the patency of the vessel. Soft tissue injury could also be assessed by extravasation of contrast medium as seen in a case with an agonal bruise on the forehead (Fig. 8). In addition to the detection of stenosis, its density and composition could be correlated to the histological appearance and showed hyperdense calcification parts and hypodense fatty areas (Fig. 6). For more detailed explanation see the figure legends.

Discussion

Method and Literature

Postmortem angiography has a long history and goes back to the early decades of the twentieth century (41–46). The existing literature is based on traditional autopsies as it was used to investigate the vascular systems of isolated organs, such as the heart (16–24,31,37,38,41,44,46–100), the brain (29,30,32,34,36,101–112), the lung (113,114), the kidneys (45), the spleen (33), the intestine (27,115–117), the uterus (118), the spinal column (119) and the extremities (120,121). Exceptions to this are postmortem angiographic investigations of fetuses and newborn babies (39,43, 122–128) as they predominantly utilized the umbilical vessels for injection of the radiopaque contrast agent without previous autopsy. Impressively, these studies imaged the entire arterial system of the fetus and this triggered the idea to transfer this minimally invasive angiographic approach onto adult human corpses in order to assess the vascular pathology within the concept of a minimally invasive autopsy (1).

Contrary to fetuses and newborn babies, adult human corpses do not present with an existing vascular access. Therefore, an access to the arterial system must be created and we used two small inguinal incisions. We deemed this as acceptable, as similar incisions are performed in embalming or conservation procedures, which both aim at keeping the body intact (129–131). Future alternatives might be less invasive by using semiautomatic image-guided puncture systems; these have not been implemented yet to reach the aortic arch for the injection of the contrast agents (132–134). When these

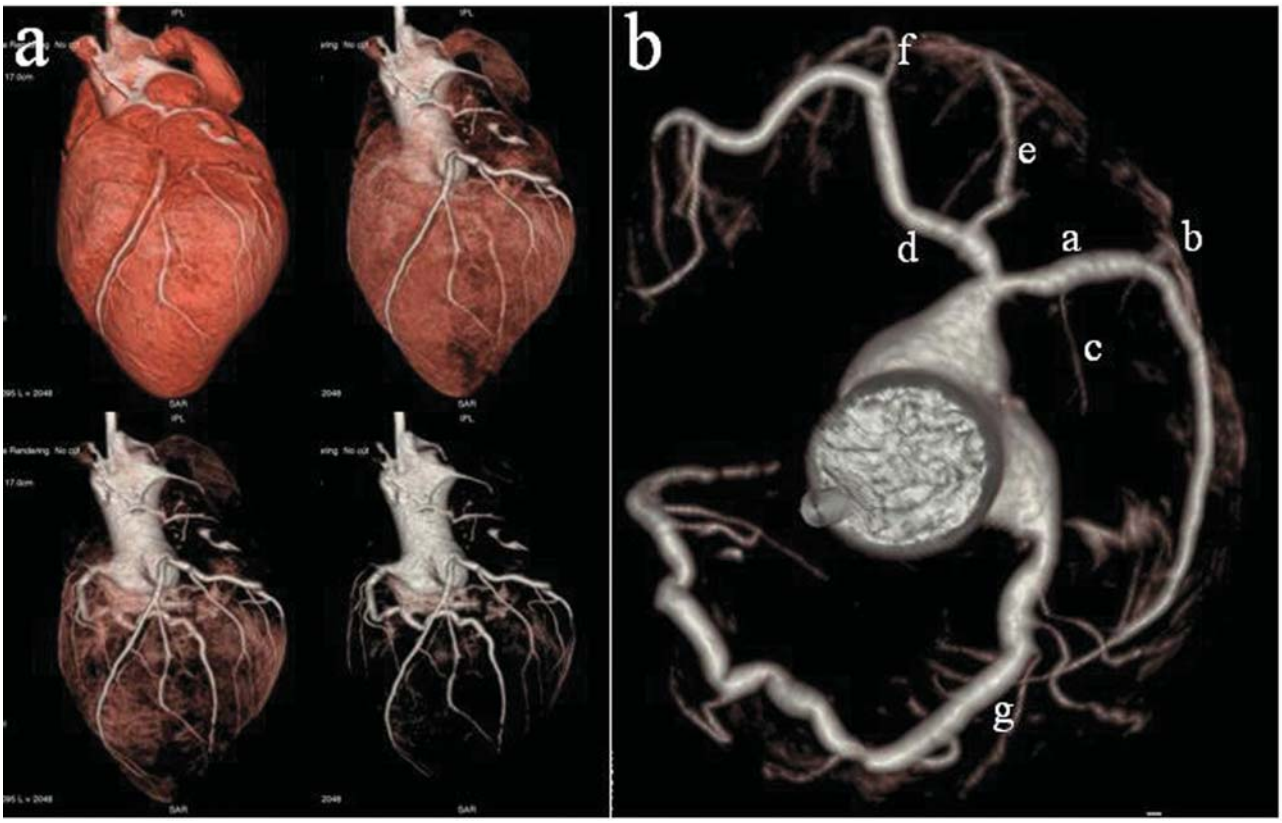

FIG. 3—*Postmortem coronary MSCT angiography in the ex-vivo porcine model: (a) The 4 images show an oblique anterior-posterior 3D volume rendering view with successive exclusion of the soft tissue within the reconstructed volume. Injection of the meglumine-ioxithalamate was performed into the aortic root. (b) Cranio-caudal view of the reconstructed coronaries: a-left anterior descending coronary artery (LAD), b-first diagonal branch, c-first septal perforator, d-circumflex coronary artery (CX), e-first posterolateral branch, f-second posterolateral branch and g-right coronary artery.*

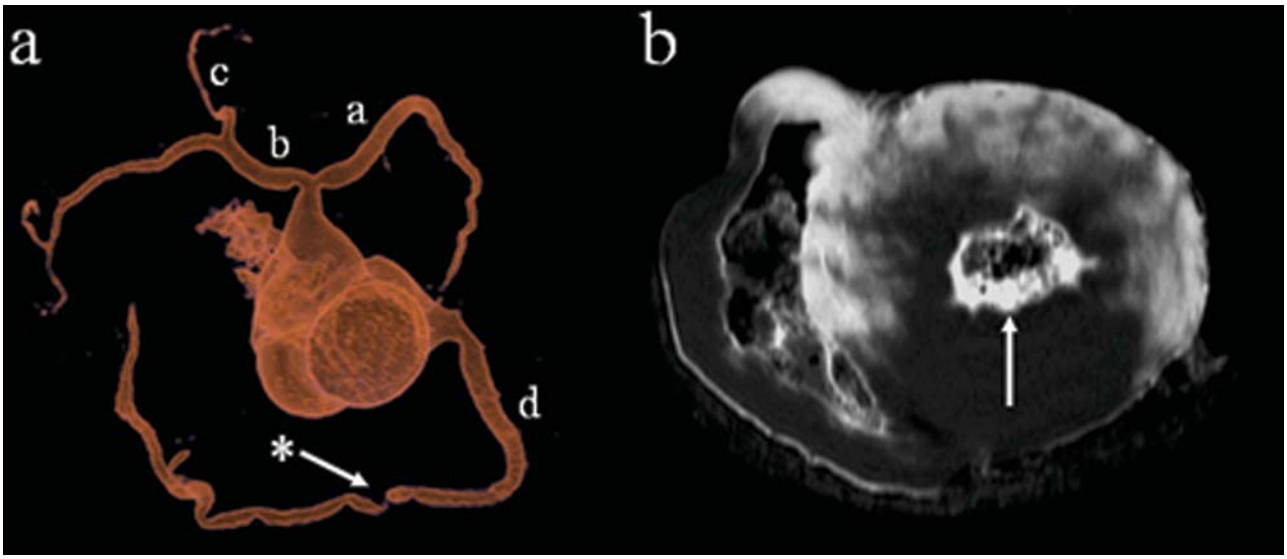

FIG. 4—*Postmortem coronary MRI angiography in the ex-vivo porcine model: (a) Cranio-caudal view of a 3D VR reconstruction of the porcine coronary artery system with the gadolinium solution injected into the aortic root: a-left anterior descending coronary artery, b-circumflex coronary artery, c-first posterolateral branch and d-right coronary artery. Specimen contained small amounts of air due to the slaughtering procedure that caused contrast agent defects within the vessel and thereby simulate occlusion of the right coronary artery (∗). (b) Short axis T1-weighted image (TE-15 ms/TR-400 ms) after selective injection of the left main coronary artery. It visualizes the myocardial distribution of the contrast agent depending on the anatomy of the left main coronary artery. Slight insufficiency of the aortic valve caused backflow of contrast agent into the left ventricle (arrow).*

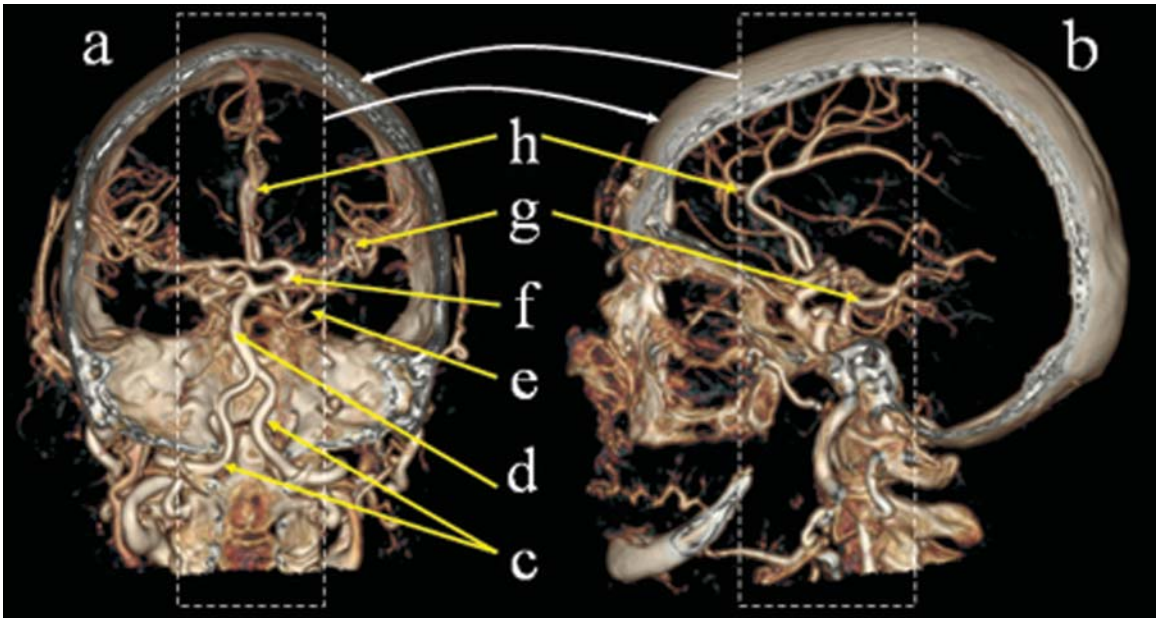

FIG. 5—*Cranial 3D volume rendered MSCT angiography (same case as in Fig. 8): (a) Posterior-anterior view visualizes the intracranial arterial system on a slab of the whole data set; slab thickness and orientation is indicated in b (dashed frame). (b) Lateral view on a cranial slab of the same data set as in a; slab thickness and orientation is indicated in a (dashed frame). Note the vertebral arteries (c), the basilar artery (d), a small posterior cerebral artery (e), the arterial circle of Willis (f), anterior cerebral artery-pericallosal artery (h) and middle cerebral artery (g).*

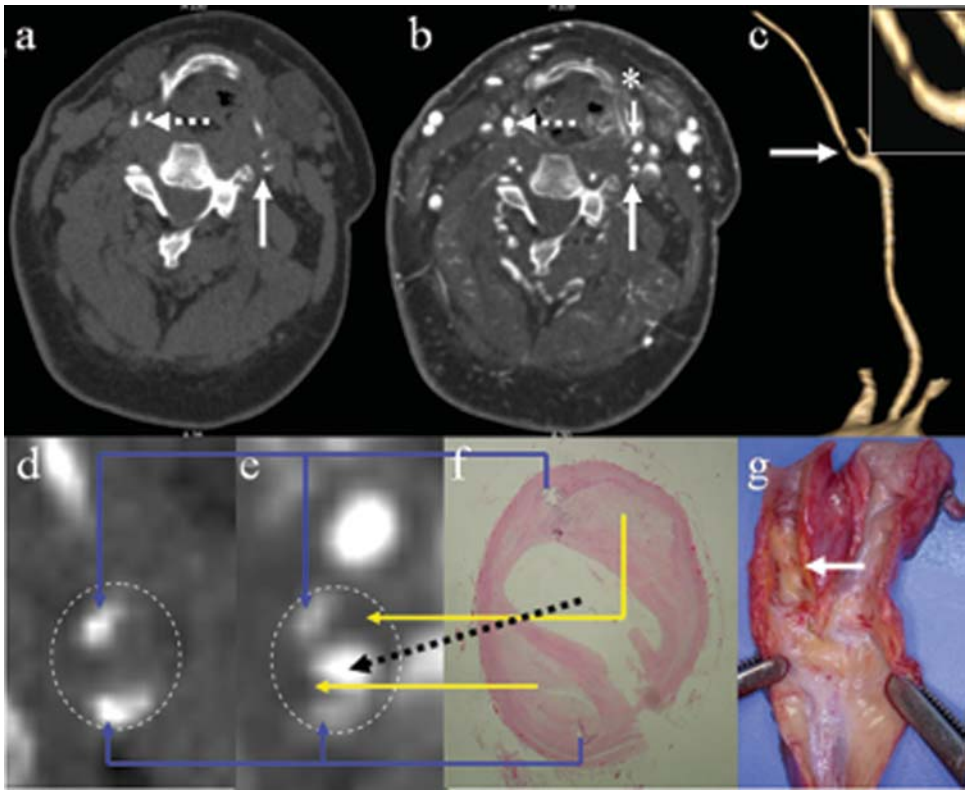

FIG. 6—*Human left internal carotid artery stenosis (same case as in Fig. 7): (a) Native axial MSCT image shows two calcifications within the wall of the left internal carotid artery (arrow). Right common carotid artery also shows calcifications (dashed arrow). (b) Postcontrast axial MSCT image visualizes the lumen of the left internal carotid artery distinctively narrowed between both calcifications (arrow) compared to the left external carotid artery (∗). Angiography of the right common carotid artery reveals a normal lumen (dashed arrow). (c) 3D volume rendered reconstruction of the left carotid artery illustrates the narrowing just above the bifurcation. (d) Magnification of the left internal carotid artery (dashed circle) in Fig. 6a. (e) Magnification of the left internal carotid artery (dashed circle) in Fig. 6b. (f) Histological cross section (H&E) of the presented stenosis. Calcifications (blue arrows) appear dense and therefore white within the vessel wall at MSCT (Fig. 6d,e). The lipid rich core of the lesions (yellow arrows) appears dark at MSCT (Fig. 6e) as the density of fat (∼−100 Hounsfield Units/HU) is distinctively lower than that of other soft tissue (0–100 HU). The narrowed lumen (black dashed arrow) is bright at MSCT due to the radiopaque contrast agent. (g) Autoptical appearance of the stenosis is shown.*

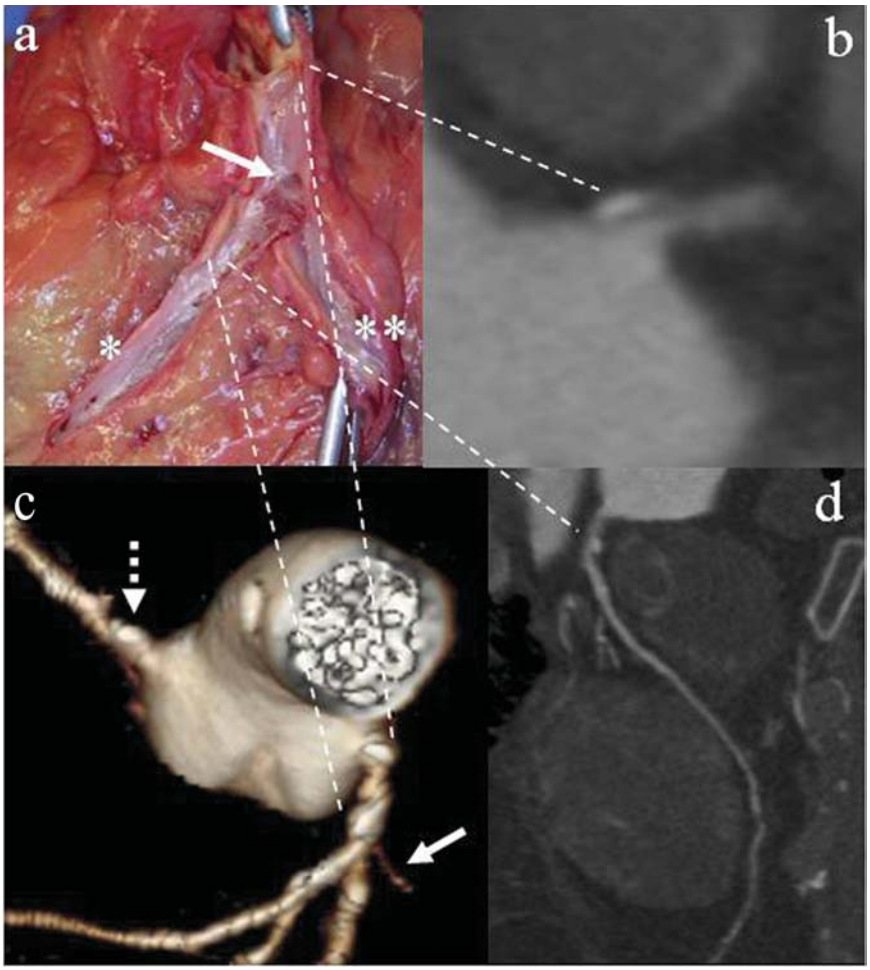

FIG. 7—*Human coronary MSCT angiography (same case as in Fig. 6): (a) Autoptical appearance of the coronary anatomy in this case with a branching of the left main coronary artery into a LAD (∗), a major intermediate branch (∗∗) and a small CX (arrow). Calcifications of the left orifice and within the proximal LAD cause narrowing of the vessel. (b) Reformatted MSCT data of the left orifice visualize the calcification and the moderate narrowing of the lumen. (c) 3D volume rendered aortic root and coronary arteries in a cranio-caudal view visualizes the lumen and the mural calcifications of the left coronary artery correlated to Fig. 7a. Due to the calcifications no assessment of the coronary lumen can be made. Note additional calcifications within the right coronary artery (dashed arrow) and the very small CX (arrow). (d) Curved reformatted MSCT data of the LAD show the vessel wall lesion as narrowing the vessel lumen. Nevertheless as nowhere totally occluding the LAD its distal segments are well visualized and show no further pathology.*

technical challenges are overcome, the open preparation procedure, as presented here, will become obsolet.

Contrary to our own expectations it was in all of the 3 cases possible to get the flexible tube via the femoral and iliac artery through the abdominal aorta into the aortic arch. In two of the three corpses the procedure was slightly complicated by severe atherosclerosis of the iliac artery. But the technique as described in material and methods could easily overcome this problem.

The access via the femoral artery has the disadvantage of necessitating a severing of the femoral artery before angiography is performed as a tight ligation is needed to fix the tube within the vessel. This current problem should also be overcome when the technical conditions for an automated transthoracic puncture are implemented. A possible method is the puncture of the ascending aorta under image guidance through upper intercostal spaces, thus simplifying the method. In the second vascular access for the pressure control, a T-piece with two ligations was inserted, thus allowing the contrast medium to reach the periphery of the second leg (Fig. 1*c*). This might also soon be obsolete, when a puncture for the placing of a pressure measurement probe will be possible.

Discussing the minimal invasiveness of the approach, we questioned whether the visualization of the coronary arteries is sufficient for diagnostic purposes without separate intubation and injection of contrast medium in each coronary orifice. As long as an intra aortic pressure that reliably presses the contrast medium through the coronaries can be achieved, a selective orifice intubation may not to be necessary. In the literature, several studies have shown adequate results in coronary and bypass graft visualization by injecting the contrast medium into the aortic root (60,62,93). Selective intubation of the coronaries may result in an increased image quality but will no longer be practicable in a minimally invasive manner. This problem will be nearly intractable when aorto-coronary bypass grafts need to be investigated. Injected into the ascending aorta with a low physiological arterial pressure of 50–60 mmHg, the contrast medium will distribute within the entire arterial system including unknown bypass grafts.

Injection Pressure

In the literature different injection pressures are advised. Contrast media of increased viscosity require an elevated injection pressure as compared to vital conditions, ranging from 150 mmHg (21,24,49) to 200 mmHg (55,59,67,115) and up to 250 mmHg (45). Aqueous contrast agents of lower viscosity need lower injection

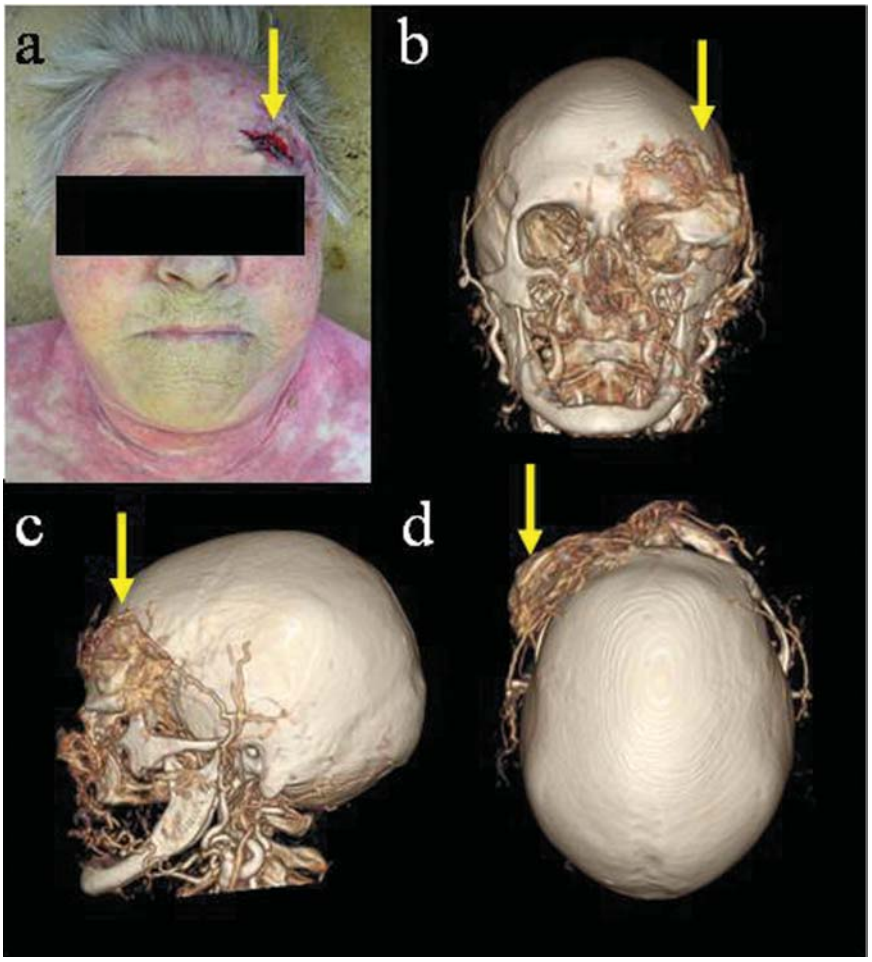

FIG. 8—*Volume rendered cranial superficial MSCT angiogram (same case as in Fig. 5): (a) An agonal crush wound was present on the left forehead (arrow). (b) Anterior-posterior view of the MSCT angiography shows massive extravasation of the contrast medium within the tissue above the left orbita. (c) Left lateral view. (d) Cranio-caudal view.*

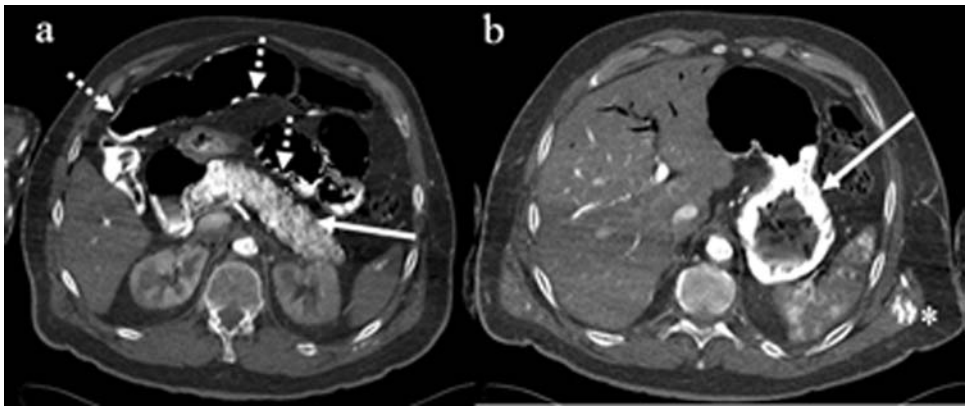

FIG. 9—*Special postmortem MSCT angiographic characteristics: (a) Demonstrated is massive enhancement of the pancreas due to autolytic vulnerability of the pancreatic capillary bed (arrow) and enhancement of the bowel wall due to beginning putrefaction (dashed arrow). Note the enhancement of the renal cortex due to increased vascularization compared to the medulla. (b) Ruptures within the vulnerable capillary bed of the gastric and bowel wall cause the contrast agent to enter the gastric or bowel lumen (arrow). Note the enhancement of an intra muscular hematoma within the left latissimus dorsi muscle (∗).*

pressures such as 120 mmHg (17,106), 100 mmHg (74) or less (135). It is not advisable to reach these high pressures when angiography of an entire corpse is performed. Especially the capillary system of the intestinal wall, being firstly exposed to the destructive putrefaction process, might not withstand "vital" pressures. Indeed, according to our experience, even at pressures of 60–70 mmHg the contrast medium will enter the bowel wall and penetrate into the intestinal lumen or cause a diffuse enhancement of the autolytic pancreas (Fig. 9). If the injection pressure is further increased, a relevant volume of contrast medium might get lost

within the intestine and cause different artifacts. Therefore, the maximal intravascular pressure during injection should be progressively reduced with increasing postmortem interval. In other words, angiographic investigations should probably be performed as early as possible after death.

Injected Contrast Agent Volume

The volume to be injected is certainly larger than for single organ or fetal angiography. To fill the entire arterial system unto the periphery, the injected volume needs to be more than the expected arterial volume of the corpse. The contrast agent might also enter the pulmonary veins due to regurgitation in insufficient aortic and mitral valves. Thereby, further volume may get lost. To inject volumes distinctively larger than the arterial volume results in a venous overlap that will complicate image interpretation and should therefore be avoided. In our experience it is advisable to start with volumes between 1–2 L, adapted to the sex and habitus of the corpse and to eventually add an increasing volume through an additional injection.

Contrast Agents

In the past different radiopaque agents have been utilized for postmortem angiography. Barium sulphate suspended in H_2O has been very popular (16–18,38,72–77,81,83–85,102,104–107,113,118,121,123–125,127,135–138). The authors showed high quality angiographic x-ray images of the investigated vessels. As barium sulphate is available in different particle sizes, not all suspensions reach the capillary bed and this may lead to variable visualization of the capillary system. Meglumine-ioxithalamate, as used in our approach is a water soluble iodinated contrast agent (111,112), radiographic visualization of the capillary bed depends only on the sufficiency of the vascularization and the injection parameters. Nevertheless, we consider barium sulphate suspensions of adequate particle size as an applicable alternative, since our preliminary experiments on the porcine hearts included aqueous barium sulfate suspensions and were able to show comparable results to those of iodinated components—here not presented.

Nearly as often, barium sulphate was used in suspension with gelatine (19–24,45,47,49–57,60–67,70,71,80,90,101,114,115,117,122,128,139–143). This combination is suited for radiological investigation of extracted organs or organ parts as it is a thin fluid when warmed up and can easily be injected into any kind of tubular system and hardens when cooling down. Thereby the barium sulphate remains within the vessel system and can be used for angiographic or micro angiographic X-ray investigations even when the organ is further dissected or cut into thin slices. This major advantage for autopsy accompanying radiological investigations will be futile when no cutting knives are needed, as the idea of virtual autopsy intends. The usefulness of gelatine suspensions for minimally invasive investigations of an entire human corpse is further reduced by the limitation to one injection. When gelatine has hardened, the vessels are filled with a rigid medium and do not allow for an additional injection. But these additional injections are useful when small gas bubbles, whether by gas embolism or due to putrefaction, which can not be surely excluded within the corpse, occlude parts of the vascular system. Further injections move the bubbles within the vessel to the periphery and this can visualize the lumen of a vessel previously occluded by gas.

Silicon as carrier substance demonstrates similar properties as gelatine (25–36,91,93,119). Once hardened, it can display the anatomy and the lumen of the investigated vessel after autopsy when extracted from the vessel as a cast. For postmortem minimally invasive angiography this advantage is irrelevant, because a dissection of the vessel is not intended. Therefore, the limitation to one injection limits is use for the virtual approach.

Besides hydrophilic contrast media and aqueous suspensions, lipophilic contrast media or oily suspensions have been used for different reasons to visualize the vascular system on postmortem X-rays (41,68,69,89,94–96,116,120). These media leave the vascular system within the capillary bed to a distinctively lesser degree, thus enabling a postmortem circulation using a peristaltic pump. Thereby angiographic investigations of the arterial, parenchymic and venous system might be possible (144,145). Comparison of both types of contrast agents showed that lipophilic contrast media systematically visualized larger diameters of investigated vessels compared to aqueous media (146). Additionally the investigated vessel diameter showed an increased standard deviation when lipophilic media were used (146). This may be a result of increased injection pressure caused by an increased viscosity, as compared to the aqueous solutions and higher pressure may inflate the postmortem vessel diameter more during and after injection. As a further reason for a systematic overestimation of the diameter, the interaction of vessel wall and lipophilic agents has to be discussed. Especially in vessel regions with atherosclerotic plaques and stenosis these media easily enter the vessel wall and solve the deposed lipids such as cholesterol (147). This leads to extravasations of the contrast medium into the plaque and causes diagnostic problems in assessment of the reduction of the vessel lumen particularly in those regions where angiography needs to be a definite diagnostic tool to gain routine application.

Furthermore, lipophilic media show an increased temperature dependence of their viscosity causing alternating injection pressures in contrast to the constantly low viscosity of the hydrophilic media within the range of usual corpse temperatures (0°C–40°C) (147).

Aqueous media have the minor disadvantage of partly leaving the vascular capillary bed system and entering the interstitial tissue. To assess vascular morphology the CT-scan has to be performed immediately after injection has stopped as long as the applied pressure results in a "vital" shape of the arterial vessels avoiding collapsed vessels in dorsal regions of the corpse. Interstitial accumulation of the contrast media can result in histological signs of edema. As long as imaging is used in a combination of MRI and MSCT, the differentiation between real edema and angiographic artifacts can be made by assessing the native predominantly T2-weighted MRI scans for preexisting edema. Secondly, a comparison of the native MSCT scan with MSCT angiography will reveal tissue around vessels that accumulates contrast medium. In particular the ability of aqueous agents to pass the capillary bed offers the possibility to assess vascular territories with different tissue distribution depending on the sufficiency of the corresponding arterial vessel. As shown in the ex-vivo porcine model, contrast distribution within the myocardium reveals the coronary anatomy. We hypothesize, that local areas of missing myocardial contrast might reflect occluded coronaries in postmortem minimally invasive angiography.

A final comment to contrast media may be made: the agents used in our approach do not leave the corpse nor do they interfere with postmortem procedures such as cremation, avoiding an environmental pollution on local cemeteries.

Results and Perspectives

The presented method is not restricted to the detection of stenosis or plaques but also can detect injuries, showing external or internal extravasation of the contrast agent. Elaborate preparations to find

the bleeding source might be replaced by a short radiological investigation. This application might gain special importance in the visualization of soft tissue injuries such as small liver or spleen ruptures. The detection of tiny hemorrhages, as often encountered in tumor lesions and often missed in a classical autopsy, may be facilitated. Unenhanced postmortem imaging is currently not able to display small tissue lesions with readapted wound margins. Postmortem angiography may therefore detect previously missed lesions.

As shown within the ex-vivo porcine model, postmortem angiography based on magnetic resonance imaging provides nearly comparable results (Fig. 4). The major drawback of MRI in postmortem angiography is the distinctively longer acquisition time. Especially for whole body angiography MSCT is currently faster, although parallel imaging will allow for a fast whole body MR examination in the near future (148,149). Furthermore MSCT allows the acquisition of thinner slices down to 0.5 mm that result in an increased quality of the performed 3D reconstructions. It is therefore likely that in the near future MSCT will be more important for postmortem angiography than MRI, supported by the lower cost of contrast agents for MSCT. But MRI may serve as an alternative tool for detailed vascular questions, e.g. when calcified plaques and the vascular lumen can not be distinguished by MSCT. It may solve the problem by selectively enhancing the lumen and thereby distinguishing it from the calcified hypointense plaque. Studies have already shown that MRI is able to further discriminate the different micro structural components of an atherosclerotic plaque, such as lipids or fibro cellular tissue (150–154). Thereby, in MSCT detected lesions can be further investigated using the more elaborate but increased soft tissue resolution providing MRI technique. Especially postmortem minimally invasive cardiac diagnostics depends on vessel lumen assessment (11,155). Compared to the clinical MSCT assessment of the coronary artery disease, postmortem scans are not influenced by cardiac motion and ventilation and thereby acquire images of increased quality.

We consider postmortem angiography primarily as a technique for the detection of macroscopic vascular pathologies, such as occlusions, stenosis or plaques. We assume that the definite diagnosis will often require histological investigation of the detected vascular alteration. Therefore image-guided biopsy has to be implemented in addition to postmortem angiography to maintain the minimally invasive autopsy.

Limitations of our approach are currently manifold: the low number of subjects in our initial experiments requires further studies with a larger spectrum of pathology to prove the reliability of the method. Forensic cases with major vessel injuries, such as seen in fatal hemorrhage, might prevent the required intravascular injection pressure. Cases presenting in an advanced stage of decay will limit the application of the postmortem angiography twofold; putrefaction gas will lead to intravascular artifacts and the injection pressure has to be decreased in view of the vulnerability of vessels predominantly in the mesenteric territory. Also, the introduced approach is clearly limited to systemic arterial diseases, whether a modification of the injection may have to be adapted for the detection of venous or pulmonary artery diseases.

Summary

Initial experiments using a porcine model were performed to display the coronary artery system. On three human corpses minimal invasive angiographic examinations were carried out. The anatomy of the arterial system was well displayed including the intracranial branches as well as the coronary branches. Stenosis and calcified plaques were detected. A soft tissue injury showed severe contrast agent extravasation. Limitations of the method are advanced stages of decay and causes of death with major vessel injury (e.g., rupture of aorta).

Conclusion

The first step to a minimal invasive postmortem assessment of the vascular pathology has been made. Especially the detection of minor bleeding sources will be simplified using the introduced approach.

Acknowledgments

We are particularly grateful to Urs Königsdorfer and Roland Dorn (both Institute of Forensic Medicine, University of Bern) for their experienced support in innumerable varying ways. Thanks go further to Therese Perinat (Institute of Forensic Medicine) for the preparation of the tissue specimen and to Susanne Boemke as well as Kati Haenssgen (both Institute of Human Anatomy, University of Bern) for the reliable collaboration. Furthermore we would like to express our gratitude to Verena Beutler and Karin Zwygart (Department of Clinical Research, Magnetic Resonance Spectroscopy and Methodology, University of Bern) for their assistance during the data acquisition in MRI. The authors also thank Andreas Hofer (Medical Technology Department, Inselspital, Bern) for the technical support and Dr. med. Stephan Bolliger for the support in manuscript preparation.

References

1. Thali MJ, Yen K, Schweitzer W, Vock P, Boesch C, Ozdoba C, Schroth G, Ith M, Sonnenschein M, Doernhoefer T, Scheurer E, Plattner T, Dirnhofer R. Virtopsy, a new imaging horizon in forensic pathology: virtual autopsy by postmortem multislice computed tomography (MSCT) and magnetic resonance imaging (MRI)-a feasibility study. J Forensic Sci 2003;48(2):386–403. [PubMed]
2. Thali MJ, Yen K, Plattner T, Schweitzer W, Vock P, Ozdoba C, Dirnhofer R. Charred body: virtual autopsy with multi-slice computed tomography and magnetic resonance imaging. J Forensic Sci 2002;47(6):1326–31. [PubMed]
3. Thali MJ, Schweitzer W, Yen K, Vock P, Ozdoba C, Spielvogel E, Dirnhofer R. New horizons in forensic radiology: the 60-second digital autopsy-full-body examination of a gunshot victim by multislice computed tomography. Am J Forensic Med Pathol 2003;24(1):22–7. [PubMed]
4. Shiotani S, Kohno M, Ohashi N, Yamazaki K, Nakayama H, Watanabe K, Itai Y. Dilatation of the heart on postmortem computed tomography (PMCT): comparison with live CT. Radiat Med 2003;21(1):29–35. [PubMed]
5. Shiotani S, Kohno M, Ohashi N, Yamazaki K, Nakayama H, Watanabe K, Oyake Y, Itai Y. Non-traumatic postmortem computed tomographic (PMCT) findings of the lung. Forensic Sci Int 2004;139(1):39–48. [PubMed]
6. Bisset RA, Thomas NB, Turnbull IW, Lee S. Postmortem examinations using magnetic resonance imaging: four year review of a working service. BMJ 2002;324(7351):1423–4. [PubMed]
7. Patriquin L, Kassarjian A, Barish M, Casserley L, O'Brien M, Andry C, Eustace S. Postmortem whole-body magnetic resonance imaging as an adjunct to autopsy: preliminary clinical experience. J Magn Reson Imaging 2001;13(2):277–87. [PubMed]
8. Wallace SK, Cohen WA, Stern EJ, Reay DT. Judicial hanging: postmortem radiographic, CT, and MR imaging features with autopsy confirmation. Radiology 1994;193(1):263–7. [PubMed]
9. Farkash U, Scope A, Lynn M, Kugel C, Maor R, Abargel A, Eldad A. Preliminary experience with postmortem computed tomography in military penetrating trauma. J Trauma 2000;48(2):303–8. [PubMed]
10. Donchin Y, Rivkind AI, Bar-Ziv J, Hiss J, Almog J, Drescher M. Utility of postmortem computed tomography in trauma victims. J Trauma 1994;37(4):552–5. [PubMed]

11. Jackowski C, Schweizer W, Thali M, Yen K, Aghayev E, Sonnenschein M, Vock P, Dirnhofer R. Virtopsy: Postmortem imaging of the human heart in situ using MSCT and MRI. Forensic Sci Int 2005;149(1):11–23. [PubMed]
12. Aghayev E, Yen K, Sonnenschein M, Ozdoba C, Thali M, Jackowski C, Dirnhofer R. Virtopsy post-mortem multi-slice computed tomograhy (MSCT) and magnetic resonance imaging (MRI) demonstrating descending tonsillar herniation: comparison to clinical studies. Neuroradiology 2004;46(7):559–64. [PubMed]
13. Jackowski C, Thali M, Sonnenschein M, Aghayev E, Yen K, Dirnhofer R, Vock P. Visualization and quantification of air embolism structure by processing postmortem MSCT data. J Forensic Sci 2004;49(6):1339–42. [PubMed]
14. Thali M, Vock P. Role of and techniques in forensic imaging. In: Payen-James J, Busuttil A, Smock W, editors. Forensic medicine: clinical and pathological aspects. London: Greenwich Medical Media, 2003; 731–45.
15. Nerantzis CE, Koutsaftis PN. Variant of the left coronary artery with an unusual origin and course: anatomic and postmortem angiographic findings. Clin Anat 1998;11(6):367–71. [PubMed]
16. Schultz TC. Simple method for demonstrating coronary arteries at postmortem examination. Am J Forensic Med Pathol 1987;8(4):313–6. [PubMed]
17. Moberg A. Anastomoses between extracardiac vessels and coronary arteries. II. Via internal mammary arteries. Post-mortem angiographic study. Acta Radiol Diagn (Stockh) 1967;6(3):263–72. [PubMed]
18. Nerantzis C, Avgoustakis D. An S-shaped atrial artery supplying the sinus node area. An anatomical study. Chest 1980;78(2):274–8. [PubMed]
19. Thomas AC, Davies MJ. Post-mortem investigation and quantification of coronary artery disease. Histopathology 1985;9(9):959–76. [PubMed]
20. Thomas AC, Pazios S. The postmortem detection of coronary artery lesions using coronary arteriography. Pathology 1992;24(1):5–11. [PubMed]
21. Robbins SL, Solomon M, Bennett A. Demonstration of intercoronary anastomoses in human hearts with a low viscosity perfusion mass. Circulation 1966;33(5):733–43. [PubMed]
22. Rodriguez FL, Robbins SL. Postmortem angiographic studies on the coronary arterial circulation; intercoronary arterial anastomoses in adult human hearts. Am Heart J 1965;70:348–64. [PubMed]
23. Weiler G, Knieriem HJ. Contribution to the morphometry of coronary arteriosclerosis (author's transl). Z Rechtsmed 1975;75(4):241–51. [PubMed]
24. Levin DC, Fallon JT. Significance of the angiographic morphology of localized coronary stenoses: histopathologic correlations. Circulation 1982;66(2):316–20. [PubMed]
25. Karhunen PJ, Mannikko A, Penttila A, Liesto K. Diagnostic angiography in postoperative autopsies. Am J Forensic Med Pathol 1989; 10(4):303–9. [PubMed]
26. Kauppila LI. Blood supply of the lower thoracic and lumbosacral regions. Postmortem aortography in 38 young adults. Acta Radiol 1994; 35(6):541–4. [PubMed]
27. Segerberg-Konttinen M. Demonstration of esophageal varices postmortem by gastroesophageal phlebography. J Forensic Sci 1987; 32(3):703–10. [PubMed]
28. Kauppila LI. Prevalence of stenotic changes in arteries supplying the lumbar spine. A postmortem angiographic study on 140 subjects. Ann Rheum Dis 1997;56(10):591–5. [PubMed]
29. Karhunen PJ, Penttila A, Erkinjuntti T. Arteriovenous malformation of the brain: imaging by postmortem angiography. Forensic Sci Int 1990;48(1):9–19. [PubMed]
30. Karhunen PJ. Neurosurgical vascular complications associated with aneurysm clips evaluated by postmortem angiography. Forensic Sci Int 1991;51(1):13–22. [PubMed]
31. Weman SM, Salminen US, Penttila A, Mannikko A, Karhunen PJ. Postmortem cast angiography in the diagnostics of graft complications in patients with fatal outcome following coronary artery bypass grafting (CABG). Int J Legal Med 1999;112(2):107–14. [PubMed]
32. Karhunen PJ, Kauppila R, Penttila A, Erkinjuntti T. Vertebral artery rupture in traumatic subarachnoid haemorrhage detected by postmortem angiography. Forensic Sci Int 1990;44(2–3):107–15. [PubMed]
33. Karhunen PJ, Penttila A. Diagnostic postmortem angiography of fatal splenic artery haemorrhage. Z Rechtsmed 1989;103(2):129–36. [PubMed]
34. Karhunen PJ, Servo A. Sudden fatal or non-operable bleeding from ruptured intracranial aneurysm. Evaluation by post-mortem angiography with vulcanising contrast medium. Int J Legal Med 1993;106(2):55–9. [PubMed]
35. Kauppila LI. Ingrowth of blood vessels in disc degeneration. Angiographic and histological studies of cadaveric spines. J Bone Joint Surg Am 1995;77(1):26–31. [PubMed]
36. Saimanen E, Jarvinen A, Pentitila A. Cerebral cast angiography as an aid to medicolegal autopsies in cases of death after adult cardiac surgery. Int J Legal Med 2001;114(3):163–8. [PubMed]
37. Smith M, Trummel DE, Dolz M, Cina SJ. A simplified method for postmortem coronary angiography using gastrograffin. Arch Pathol Lab Med 1999;123(10):885–8. [PubMed]
38. Prahlow JA, Scharling ES, Lantz PE. Postmortem coronary subtraction angiography. Am J Forensic Med Pathol 1996;17(3):225–30. [PubMed]
39. Russell GA, Berry PJ. Post mortem radiology in children with congenital heart disease. J Clin Pathol 1988;41(8):830–6. [PubMed]
40. Rah BR, Katz RJ, Wasserman AG, Reiner JS. Post-mortem three-dimensional reconstruction of the entire coronary arterial circulation using electron-beam computed tomography. Circulation 2001; 104(25):3168. [PubMed]
41. Parade GW. Coronardarstellung. Verh dtsch Ges inn Med 1933;45:216–20.
42. Miyata S. Aufbau und Gestalt der peripheren arteriellen Strombahn des kleinen Kreislaufs. Virchows Arch Path Anat 1939;304:608–24.
43. Hintze A. Fehlbildungen im Blutgefässsystem und ihr Nachweis mittels der Röntgenuntersuchung. Virchows Arch Pathol Anat 1933;289:705–17.
44. Schlesinger MJ. An injection plus dissection study of coronary artery occlusions and anastomoses. Am Heart J 1938;15:528–68.
45. Hinman F, Morison DM. Comparative study of circulatory changes in hydronephrosis, caseo-cavernous tuberculosis, and polycystic kidney. a preliminary report. J Urol 1924;11:131–41.
46. Crainicianu A. Anatomische Studien über die Coronararterien und experimentelle Untersuchungen über ihre Durchgängigkeit. Virchows Arch 1922;238:1–75.
47. van Dantzig JM, Becker AE. Sudden cardiac death and acute pathology of coronary arteries. Eur Heart J 1986;7(11):987–91. [PubMed]
48. Dock W. The capacity of the coronary bed in cardiac hypertrophy. J Exp Med 1941;74:177–86.
49. Falk E. Unstable angina with fatal outcome: dynamic coronary thrombosis leading to infarction and/or sudden death. Autopsy evidence of recurrent mural thrombosis with peripheral embolization culminating in total vascular occlusion. Circulation 1985;71(4):699–708. [PubMed]
50. Farb A, Tang AL, Burke AP, Sessums L, Liang Y, Virmani R. Sudden coronary death. Frequency of active coronary lesions, inactive coronary lesions, and myocardial infarction. Circulation 1995;92(7):1701–9. [PubMed]
51. Freudenberg VH, Knieriem HJ, Moller C, Janzen C. Quantitative morphology of coronary arteriosclerosis and coronary insufficiency (author's transl). Basic Res Cardiol 1974;69(2):161–203. [PubMed]
52. Galbraith JE, Murphy ML, de Soyza N. Coronary angiogram interpretation. Interobserver variability. JAMA 1978;240(19):2053–56. [PubMed]
53. Hochman JS, Phillips WJ, Ruggieri D, Ryan SF. The distribution of atherosclerotic lesions in the coronary arterial tree: relation to cardiac risk factors. Am Heart J 1988;116(5 Pt 1):1217–22. [PubMed]
54. Hutchins GM, Bulkley BH, Ridolfi RL, Griffith LS, Lohr FT, Piasio MA. Correlation of coronary arteriograms and left ventriculograms with postmortem studies. Circulation 1977;56(1):32–7. [PubMed]
55. Lagundoye SB, Edington GM, Ibeachum G, Cockshott WP. Post mortem coronary arteriography in Nigerians: a radiological review. Afr J Med Med Sci 1976;5(1):9–17. [PubMed]
56. Laurie W, Woods JD. Interarterial coronary anastomoses in three race groups. Lancet 1962;1:13–7. [PubMed]
57. Pepler WJ, Meyer BJ. Interarterial coronary anastomoses and coronary arterial pattern. A comparative study of South African Bantu and European hearts. Circulation 1960;22:14–24. [PubMed]
58. Plachta A, Thompson SA, Speer FD. Pericardial and myocardial vascularization following cardiopericardiopexy; magnesium silicate technique. AMA Arch Pathol 1955;59(2):151–61. [PubMed]
59. Prinzmetal M, Kayland S, Margoles C, Tragerman L J. A quantitative method for determining collateral coronary corculation. J Mt Sinai Hosp N Y 1942;8:933–45.
60. Rissanen VT. Double contrast technique for postmortem coronary angiography. Lab Invest 1970;23(5):517–20. [PubMed]

61. Rozenberg VD, Nepomnyashchikh LM. Pathomorphology of myocardial bridges and their role in the pathogenesis of coronary disease. Bull Exp Biol Med 2002;134(6):593–6. [PubMed]
62. Schoenmackers J. Die Angiomorphologie der Koronarangiogramme. Roentgenfortschritte 1965;102:349–68.
63. Schoenmackers J, Bultmann FJ, Dechene G. Comparative planimetric and stereoscopic analysis of postmortal coronarogrammes. Z Kardiol 1974;63(8):689–97. [PubMed]
64. Trask N, Califf RM, Conley MJ, Kong Y, Peter R, Lee KL, Hackel DB, Wagner GS. Accuracy and interobserver variability of coronary cineangiography: a comparison with postmortem evaluation. J Am Coll Cardiol 1984;3(5):1145–54. [PubMed]
65. Weiler G, Erkrath KD, Risse M. Contribution to anastomotic coronary circulation illustrated by a Bland-White-Garland-syndome in an adult (author's transl). Z Kardiol 1979;68(10):717–9. [PubMed]
66. Weitzman D. Post-mortem coronary arteriography and its correlation with electrocardiography. Br Heart J 1964;26:330–6. [PubMed]
67. Allison RB, Rodriguez FL, Higgins EA, Jr., Leddy JP, Abelmann WH, Ellis LB, Robbins SL. Clinicopathologic correlations in coronary atherosclerosis. four hundred thirty patients studied with postmortem coronary angiography. Circulation 1963;27:170–84. [PubMed]
68. Barmeyer J. [Post mortem coronary angiography and perfusion of normal and diseased hearts, perfusibility of intercoronary anastomoses]. Beitr Pathol Anat 1968;137(4):373–90. [PubMed]
69. Barmeyer J, Reindell H. Intercoronary anastomoses in postmortum angiography. Radiologe 1971;11(5):198–202. [PubMed]
70. Bellman S, Frank HA. Intercoronary collaterals in normal hearts. J Thorac Surg 1958;36(4):584–603. [PubMed]
71. Bulkely BH, Hutchins GM. Myocardial consequences of coronary artery bypass graft surgery. The paradox of necrosis in areas of revascularization. Circulation 1977;56(6):906–13. [PubMed]
72. Coghill SB, Nicoll SM, McKimmie A, Houston I, Matthew BM. Revitalising postmortem coronary angiography. J Clin Pathol 1983;36(12):1406–9. [PubMed]
73. Davis NA. A radioisotope dilution technique for the quantitative study of coronary artery disease postmortem. Lab Invest 1963;12:1198–203. [PubMed]
74. Estes EH, Jr., Entman ML, Dixon HB, Hackel DB. The vascular supply of the left ventricular wall. Anatomic observations, plus a hypothesis regarding acute events in coronary artery disease. Am Heart J 1966;71(1):58–67. [PubMed]
75. Giraldo AA, Higgins MJ, Humes JJ. Anatomical methods in the study of cardiovascular pathology: a refined technique. Ann Clin Lab Sci 1986;16(1):13–25. [PubMed]
76. Giraldo AA, Higgins MJ. Laboratory methods in the study of coronary atherosclerosis. Pathol Annu 1988;23 Pt 1:217–36. [PubMed]
77. Gray CR, Hoffman HA, Hammond WS, Miller KL, Oseasohn RO. Correlation of arteriographic and pathologic findings in the coronary arteries in man. Circulation 1962;26:494–9. [PubMed]
78. McNamara JJ, Molot MA, Stremple JF, Cutting RT. Coronary artery disease in combat casualties in Vietnam. JAMA 1971;216(7):1185–7. [PubMed]
79. Muller-Mohnssen H. [Topography of septal arteries in the human heart and its significance in the origin of collateral circulation in coronary sclerosis.]. Beitr Pathol Anat 1957;118(1):121–42. [PubMed]
80. Murphy ML, Galbraith JE, de Soyza N. The reliability of coronary angiogram interpretation: an angiographic-pathologic correlation with a comparison of radiographic views. Am Heart J 1979;97(5):578–84. [PubMed]
81. Nerantzis CE, Koutsaftis PN. Variant of the left coronary artery with an unusual origin and course: anatomic and postmortem angiographic findings. Clin Anat 1998;11(6):367–71. [PubMed]
82. Nerantzis CE, Lefkidis CA, Smirnoff TB, Agapitos EB, Davaris PS. Variations in the origin and course of the posterior interventricular artery in relation to the crux cordis and the posterior interventricular vein: an anatomical study. Anat Rec 1998;252(3):413–7. [PubMed]
83. Nerantzis CE, Marianou SK. Ectopic "high" origin of both coronary arteries from the left aortic wall: anatomic and postmortem angiographic findings. Clin Anat 2000;13(5):383–6. [PubMed]
84. Oosawa K. Clinicopathological studies on the coronary circulation with postmortem coronary angiography. Gunma J Med Sci 1967;16(3):146–76. [PubMed]
85. Schwartz JN, Kong Y, Hackel DB, Bartel AG. Comparison of angiographic and postmortem findings in patients with coronary artery disease. Am J Cardiol 1975;36(2):174–8. [PubMed]
86. Eusterman JH, Achor RWP, Kincaid OW, Brown AL. Atherosclerotic disease of the coronary arteries. A pathologic-radiolgic correlative study. Circulation 1962;26:1288–95.
87. Farrer-Brown G, Rowles PM. Vascular supply of interventricular septum of human heart. Br Heart J 1969;31(6):727–34. [PubMed]
88. Fulton WF. Arterial anastomoses in the coronary circulation. i. anatomical features in normal and diseased hearts demonstrated by stereoarteriography. Scott Med J 1963;143:420–34. [PubMed]
89. Giese W. Anastomoses of coronary arteries in coronary arteriosclerosis. Dtsch Med Wochenschr 1957;82(17):602–4. [PubMed]
90. Heard BE. Pathology of hearts after aortocoronary saphenous vein bypass grafting for coronary artery disease, studied by post-mortem coronary angiography. Br Heart J 1976;38(8):838–59. [PubMed]
91. Jarvinen A, Manniko A, Ketonen P, Segerberg-Konttinen M, Luosto R. Surgical technique and operative mortality in coronary artery bypass. A postmortem analysis with castangiography. Scand J Thorac Cardiovasc Surg 1989;23(2):103–9. [PubMed]
92. Vesterby A. Postmortem coronary angiography and histological investigation of the conduction system of the heart in sudden unexpected death due to coronary heart disease. Acta Pathol Microbiol Scand [A] 1981;89(2):157–63. [PubMed]
93. Weman SM, Karhunen PJ, Penttila A, Jarvinen AA, Salminen US. Reperfusion injury associated with one-fourth of deaths after coronary artery bypass grafting. Ann Thorac Surg 2000;70(3):807–12. [PubMed]
94. Melnick GS, Tuna N, Gilson MJ. Postmortem coronary arteriogram. A correlation with electrocardiographic and anatomic findings. Angiology 1963;14:252–9. [PubMed]
95. van der Straten PP. La Coronarographie post mortem de l'homme age. Acta Cardiol 1955;10(1):15–43. [PubMed]
96. Brascho DJ. A technique for postmortem coronary arteriography. Am Heart J 1963;66:375–80. [PubMed]
97. Huguet JF, Luccioni R, Navarro B, Colonna J. Coronary anastomoses. Post-mortem radiographic study. Ann Radiol (Paris) 1970;13(9):651–66. [PubMed]
98. Kohlhardt M, Muller-Marienburg H, Vita G, Zeitler E. Determination of the coincidence between coronarography and pathologico-anatomical findings. Fortschr Geb Rontgenstr Nuklearmed 1963;98:399–408. [PubMed]
99. Ravin A, Geever EF. Coronary arteriosclerosis, coronary anastomoses and myocardial infarction. Arch Intern Med 1946;78(2):125–38.
100. Wexberg P, Gottsauner-Wolf M, Sulzbacher I, Birner P, Laggner A, Glogar D. Fatal late coronary thrombosis after implantation of a radioactive stent: postmortem angiographic and histologic findings–case report. Radiology 2001;220(1):142–4. [PubMed]
101. Fujikura T, Kominato Y, Shimada I, Hata N, Takizawa H. Forensic application of angiography on injured brain. Med Sci Law 1990;30(2):127–32. [PubMed]
102. Kormano M, Reijonen K. Microangiographic filling of the vascular system of the brain. Neuroradiology 1973;6(2):83–6. [PubMed]
103. Saunders RL de CH. Microangiography of the brain and spinal cord. X-raymicroscopy and microanalysis 1960;244–56.
104. Maxeiner H. Demonstration and interpretation of bridging vein ruptures in cases of infantile subdural bleedings. J Forensic Sci 2001;46(1):85–93. [PubMed]
105. Maxeiner H. Detection of ruptured cerebral bridging veins at autopsy. Forensic Sci Int 1997;89(1–2):103–10. [PubMed]
106. Hassler O. Deep cerebral venous system in man. A microangiographic study on its areas of drainage and its anastomoses with the superficial cerebral veins. Neurology 1966;16(5):505–11. [PubMed]
107. Ehrlich E, Maxheiner H, Lange J. Postmortem radiological investigation of bridging vein ruputres. Legal Med 2004;5:S225–7.
108. Dowling G, Curry B. Traumatic basal subarachnoid hemorrhage. Report of six cases and review of the literature. Am J Forensic Med Pathol 1988;9(1):23–31. [PubMed]
109. Dor P, Salamon G. The arterioles and capillaries of the brain stem and cerebellum: a microangiographic study. Neuroradiology 1970;1:27–9.
110. Mant AK. Traumatic subarachnoid haemorrhage following blows to the neck. J Forensic Sci Soc 1972;12(4):567–72. [PubMed]
111. Stein BM, McCormick W, Rodriguez JN, Taveras JM. Incidence and significance of occlusive vascular disease of the extracranial arteries as

demonstrated by post-mortem angiography. Trans Am Neurol Assoc [PubMed] 1961;86:60–6.
112. Stein BM, Svare GT. A technic of postmortem angiography for evaluating arteriosclerosis of the aortic arch and carotid and vertebral arteries. [PubMed] Radiology 1963;81:252–6.
113. Charr R, Wooddrow Savacool J. Changes in the arteries in the walls of teberculous pulmonary cavities. Arch Pathol 1940;30(6):1159–71.
114. Milne EN. Circulation of primary and metastatic pulmonary neoplasms. A postmortem microarteriographic study. Am J Roentgenol Radium [PubMed] Ther Nucl Med 1967;100(3):603–19.
115. Gloor F. Vascularization of the esophagus. Thoraxchirurgie 1953; [PubMed] 1(2):146–67.
116. Faller A. Behavior of arterial vessels in various parietal layers of the [PubMed] rectum in man. Acta Anat (Basel) 1957;30(1–4):275–86.
117. Reiner L, Rodriguez FL, Platt R, Schlesinger MJ. Injection studies on the mesenteric arterial circulation. I. Technique and observations on [PubMed] collaterals. Surgery 1959;45(5):820–33.
118. Aranyi Z, Patanyik M, Nemeth G, Scholz M, Stumpf J. Post mortem uterine arteriography and in vivo angiographic diagnosis. Acta Morphol [PubMed] Hung 1985;33(3–4):219–25.
119. Kauppila LI, Karhunen PJ, Lahdenranta U. Intermittent medullary claudication: postmortem spinal angiographic findings in two cases and in [PubMed] six controls. J Spinal Disord 1994;7(3):242–7.
120. Dejdar R, Roubkova H, Cachovan M, Kruml J, Linhart J. Comparison of postmortem angiograms with macro and microscopic findings on the A. femoralis and A. poplitea. Arch Kreislaufforsch 1967;54(3):309–35.
121. Ross CF, Keele KD. Post mortem arteriography in "normal" lower [PubMed] limbs. Angiology 1951;2(5):374–85.
122. Gronvall J, Graem N. Radiography in post-mortem examinations of fetuses and neonates. Findings on plain films and at arteriography. [PubMed] APMIS 1989;97(3):274–80.
123. Richter E. Postmortem angiocardiography in newborn infants with congenital malformation of the heart and great vessels. Pediatr Radiol [PubMed] 1976;4(3):133–8.
124. Foote GA, Wilson AJ, Stewart JH. Perinatal post-mortem radiography– [PubMed] experience with 2500 cases. Br J Radiol 1978;51(605):351–6.
125. Stoeter P, Petersen D, Voigt K. Comparative roentgenological embryology of the supraaortic arteries of domestic mammals with a prenatal angiographic technique (author's transl). Rofo 1977;126(2):150–[PubMed] 6.
126. Jeanmart L. Study of the cerebral vascularization of the human fetus by [PubMed] transumbilical angiography. Angiology 1974;25(5):334–49.
127. Beck BL. Two cases of congenital vascular malformations proved by post-mortem arteriography. Case reports. Acta Pathol Microbiol Im-[PubMed] munol Scand [A] 1987;95(1):17–21.
128. Potts DG, Svare GT, Bergeron RT. The developing brain. Correlation between radiologic and anatomical findings. Acta Radiol Diagn (Stockh) [PubMed] 1969;9:430–9.
129. Grabuschnigg P, Rous F. Preservation of human cadavers throughout history—a contribution to development and methodology. Beitr Gerichtl [PubMed] Med 1990;48:455–8.
130. Hanzlick R. Embalming, body preparation, burial, and disinterment. An overview for forensic pathologists. Am J Forensic Med Pathol [PubMed] 1994;15(2):122–31.
131. Macdonald GJ, MacGregor DB. Procedures for embalming cadavers for [PubMed] the dissecting laboratory. Proc Soc Exp Biol Med 1997;215(4):363–5.
132. Brown KT, Getrajdman GI, Botet JF. Clinical trial of the Bard CT guide [PubMed] system. J Vasc Interv Radiol 1995;6(3):405–10.
133. Fichtinger G, DeWeese TL, Patriciu A, Tanacs A, Mazilu D, Anderson JH, Masamune K, Taylor RH, Stoianovici D. System for robotically assisted prostate biopsy and therapy with intraoperative CT guidance. [PubMed] Acad Radiol 2002;9(1):60–74.
134. Masamune K, Fichtinger G, Patriciu A, Susil RC, Taylor RH, Kavoussi LR, Anderson JH, Sakuma I, Dohi T, Stoianovici D. System for robotically assisted percutaneous procedures with computed tomography [PubMed] guidance. Comput Aided Surg 2001;6(6):370–83.
135. Bohm E. Results of postmortem organ and tissue perfusions. Beitr [PubMed] Gerichtl Med 1983;41:449–58.
136. Stoeter P, Buchhocker M, Bruzek W, Drews U, Schulze K. Angiographic examinations of the circulatory development of living chick embryos (author's transl). Rofo 1980;133(1):83–91. [PubMed]
137. Bohm E. A preparative technique for morphological analysis of the vessels in head and neck for medico-legal examinations. Scan Electron Microsc 1983;(Pt 4):1973–81. [PubMed]
138. Bohm E, Hubner F. Microradiographic findings in death by hanging. Beitr Gerichtl Med 1983;41:465–73. [PubMed]
139. Hübner F, Böhm E. Zur forensischen Bedeutung postmortaler Injektions- und Perfusionstechniken. Zacchia 1985;48:95–120.
140. Rozenberg VD. Pathomorphological data of differential diagnosis if dilatational cardiomyopathy. Vrach Delo 1989;12:18–20. [PubMed]
141. Rozenberg VD. Postmortem contrast cardioventriculography. Arkh Patol 1987;49(6):82–4. [PubMed]
142. Rubin P, Casarett GW, Kurohara SS, Fujii M. Microangiography as a technique; radiation effect versus artifact. Am J Roentgenol Radium Ther Nucl Med 1964;92:378–87. [PubMed]
143. Bergquist E, Rammer L. Postmortem vertebral angiography in cases of traumatic subarachnoid hemorrhage. Radiology 1974;110(3):709–10. [PubMed]
144. Barmeyer J. [Measurement of the blood flow capacity of intercoronary anastomoses in normal pathologic heart by means of postmortal perfusion of coronary arteries]. Verh Dtsch Ges Kreislaufforsch 1968;34:381–5. [PubMed]
145. Grabher S. Postmortaler Kreislauf mit angiographischer Darstellung der arteriellen, kapillären und venösen Strombahn. Innsbruck 2004;Thesis.
146. Frik W, Persch WF. The effect of contrast media type on the vascular caliber in experimental angiography. Fortschr Geb Rontgenstr Nuklearmed 1969;111(5):620–9. [PubMed]
147. Schoenmackers J. Technik der postmortalen Angiographie mit Berücksichtigung verwandter Methoden postmortaler Gefässdarstellung. Ergebn allg Pathol Anat 1960;39:53–151.
148. Quick HH, Vogt FM, Maderwald S, Herborn CU, Bosk S, Gohde S, Debatin JF, Ladd ME. High spatial resolution whole—body MR angiography featuring parallel imaging: initial experience. Rofo 2004;176(2): 163–9. [PubMed]
149. Kramer H, Schoenberg SO, Nikolaou K, Huber A, Struwe A, Winnik E, Wintersperger B, Dietrich O, Kiefer B, Reiser MF. Cardiovascular whole body MRI with parallel imaging. Radiologe 2004;44(9):835–43. [PubMed]
150. Toussaint JF, LaMuraglia GM, Southern JF, Fuster V, Kantor HL. Magnetic resonance images lipid, fibrous, calcified, hemorrhagic, and thrombotic components of human atherosclerosis in vivo. Circulation 1996;94(5):932–8. [PubMed]
151. Wasserman BA, Smith WI, Trout HH, III, Cannon RO, III, Balaban RS, Arai AE. Carotid artery atherosclerosis: in vivo morphologic characterization with gadolinium-enhanced double-oblique MR imaging initial results. Radiology 2002;223(2):566–73. [PubMed]
152. Ruehm SG. Magnetic resonance imaging of atherosclerotic plaque. Herz 2003;28(6):513–20. [PubMed]
153. Worthley SG, Helft G, Fuster V, Fayad ZA, Rodriguez OJ, Zaman AG, Fallon JT, Badimon JJ. Noninvasive in vivo magnetic resonance imaging of experimental coronary artery lesions in a porcine model. Circulation 2000;101(25):2956–61. [PubMed]
154. Worthley SG, Helft G, Fuster V, Fayad ZA, Fallon JT, Osende JI, Roque M, Shinnar M, Zaman AG, Rodriguez OJ, Verhallen P, Badimon JJ. High resolution ex vivo magnetic resonance imaging of in situ coronary and aortic atherosclerotic plaque in a porcine model. Atherosclerosis 2000;150(2):321–9. [PubMed]
155. Jachau K, Heinrichs T, Kuchheuser W, Krause D, Wittig H, Schoening R, Beck N, Beuing O, Doehring W, Jackowski C. Computed tomography and magnetic resonance imaging compared to pathoanatomic findings in isolated human autopsy hearts. Rechtsmedizin 2004;14(2):109–16.

Additional information and reprint requests:
Christian Jackowski, M.D.
University of Bern
Institute of Forensic Medicine
IRM, Buehlstrasse 20
CH 3012 Bern
Switzerland
E-mail: christian.jackowski@irm.unibe.ch